行政院國家科學委員會專題研究計畫成果報告

以動態系統法分析母鼠發情週期之行為特性

Dynamical-System Analysis of Estrous Cycle of Mice

計畫編號：NSC 89-2213-E-002-086

執行期限：88 年 8 月 1 日至 89 年 7 月 31 日

主持人：伍次寅　　國立臺灣大學機械工程學系

共同主持人：王淑音　　中國文化大學畜產學系

計畫參與人員：張烈諄　　國立臺灣大學機械工程學系

中文摘要

本計畫以動態系統學中之非線性時間序列法來分析小母鼠生殖週期之行為特性。以每日小母鼠陰道分泌物抹片取樣中所記錄角化細胞數目變化之實驗數據作為一時間序列，應用嵌入理論中之時間延遲座標法將上述一維數據序列擴展為一動態系統於重建相空間之運動軌跡；再藉由求取此動態系統運動軌跡之 Lyapunov **指數及相關維度等不變量來分析母鼠生殖系統之生理行為模式。本研究結果證實了以僅有的一維實驗數據序列所建立之動態系統符合生理學上對於母鼠生殖系統內分泌運作機制之描述。同時，量化的資料亦顯示母鼠生殖系統之週期變化俱備一動力學中低維度之渾沌特性。**

關鍵詞：生殖週期、內分泌、非線性時間序列、動態系統、渾沌運動

Abstract

A nonlinear time-series analysis is applied in this study to investigate the dynamical behavior of the estrous cycle in mice. Taking the daily changes in the cell type distributions recorded from the vaginal smears of mice as a proper time series, a multidimensional state space can be constructed from this single-variable time series via an embedding scheme. By studying the invariant properties such as the Lyapunov exponent and the correlation dimension of the trajectories in the re-constructed state space, we can analyze the dynamics of the reproductive cycle of female mice. Present study reveals that the result from the time-series analysis is consistent with the physiological description of the reproductive endocrine system. The dynamical-system approach also suggests that the observed variation in the estrous cycle of mice is a low-dimensional chaotic motion.

Keywords: estrous cycle, endocrines, nonlinear time series, dynamical system, chaotic motion

1. Introduction

Fluctuating cycles are commonly observed in physiological phenomena, such as the cardiac rhythm in circulation, the calcium oscillation in cell biology, the glycolytic oscillation in metabolism, and the ovarian cycle in reproduction, etc. In most situations, such an oscillatory behavior does not always exhibit a simple periodic nature. In contrast to the classical principle of homeostasis [1], which states that physiological systems operate and regulate to maintain relatively stable and equilibrium-like internal states; variability and complexity in oscillation patterns have been discerned in various biochemical reactions and biological systems [2-5]. Dynamical system approach provides a promising means for understanding such complex oscillations in a qualitative as well as quantitative manner [4-6]. Particularly, the development of modern 'chaos' theory has shed much light on the origin of the apparently irregular, aperiodic oscillations found in a variety of biological and physiological contexts [2-5],[7-8]. Recent studies on the 'dynamical diseases' [4] even suggest that the dynamics of a normal healthy system is 'chaotic' while disease is featured by a more regular rhythmic behavior. This has been demonstrated

so at least in the heart rate clinics [9-10].

Mathematical modeling of physiological dynamics based on experimental observations is often fraught with difficulty. In most physical experiments, it is typical that only one or at best a few quantities are observed and measured. In some cases, the number of variables governing the behavior of the system is not even clear at the outset. These difficulties may be sidestepped by appealing to the nonlinear time series analysis specifically developed for extracting dynamics from nonlinear systems. The analysis is based on the notion that information from the dynamics of a multidimensional system is inherently embedded in the time series record of a single variable. By using a suitable unfolding technique, the trajectories and the embedding state space reconstructed from this single-variable sequence of data will have the same geometric and dynamical properties as those characterizing the actual state-space dynamics of the original system. The use of a single scalar time series to generate an embedding space and associated dynamics was suggested by Packard *et al.* [11] and was formulated into a firm theory of Embedology by Takens [12] and Casdagli, *et al.* [13].

In the past decades, the time-series analysis and the associated techniques have been used to analyze experimental data in a variety of fields, e.g., in thermo-fluid turbulence [14], in astrology [15], in cardiology [16], in epidemiology [17], in psychophysiology [18], and in economy [19], etc. In this paper, we apply the technique to study the estrous cycle of the reproductive system of mice. The endocrinology of the reproductive cycle in mammals is well understood by physiologists. However, fluctuations in the cyclicity were observed and documented. Various attempts, though inconclusive, have been made to explain such variability on a physiological basis (e.g., [20]). In the present study, we tackle the problem from the dynamical system approach. First, the hormone function in the reproductive endocrine system is briefly reviewed in the next section. Establishment of a proper single-variable experimental time series characterizing the phenomenology of the estrous cycle of mice is described in section 3. Methods and results of generating the state-space dynamics from the scalar time series of experimental observations are summarized in section 4. Feasible physiological interpretations of the present dynamical-system results are discussed in section 5.

2. Physiological description of the reproductive cycle

All female mammals show in their lifetime a reproductive period that begins from the puberty and ends with the menopause. In non-seasonal breeding animals, most female show regular physiological change repetitively unless they are pregnant. The repeated cycle of change is called the estrous cycle. Most mammals except human will estrus once in a cycle. The length of the cycle is not consistent, and is affected by species, genetics, age, environment and physiological conditions [20-22]. The estrous cycle of female mice ranges from 3 to 9 days with the average of 4-5 days. The cycle can be divided into proestrus, estrus, metestrus and diestrus stages depending on the changes of ovary, reproductive ducts and the endocrine [23-24]. During the proestrus, ovarian follicles develop rapidly and produce estrogen as stimulated by the follicular stimulating hormone (FSH) secreted by pituitary. Estrogen production increases as the size of follicles increase and affects the growth of female reproductive ducts. Proestrus lasts for roughly 12 hours, and is followed by estrus. Female mice will be in estrus and will allow copulation in this stage. A peak production of estrogen in the estrus stage causes a luteinizing hormone (LH) surge in pituitary, which leads to the ovulation of follicles. The estrus stage of mice normally lasts for 9-15 hours. After the ovulation, the corpus luteum is formed and begins to secret progesterone. This stage is called metesturs, which lasts for only 6 hours approximately. In the diestrus stage, the corpus luteum, as stimulated by the LH from pituitary, continues to grow and secrets progesterone. Progesterone increases the thickness of the endometrium and stimulates the development of the uterine gland preparing for the pregnancy to occur. If the animal is not pregnant, luteolysis occurs and a new cycle is initiated. The diestrus stage is the longest stage among the cycle and lasts for about one half of the total length of the cycle.

Theoretically, the estrous cycle can be monitored by observing the variations in the plasma hormone profiles. However, frequent bleeding not only is time consuming, it also causes stress to the animal. Moreover, the volume of the blood sample in each bleeding is too little for a practical analysis. It is pointed out [23] that in most female mammals, a morphological change in

the epithelial tissue of vagina is accompanied with the change of endocrine during the estrus cycle. In short cycling animal such as mice, the change of cell type can be observed and recorded via vaginal smears. Thus vaginal smears can be taken to establish the length of the estrous cycle and to estimate the duration of each stage.

3. Material and methods

Animals:

Ten female mice (C57BL/6J) were individually caged and raised in an animal room (21-25 ℃, 12L:12D) and fed ad libitum. After their vaginal opening, vaginal smears were done daily between 13:30 to 14:30 until their menopause (12-14 months).

Vaginal smears:

A drop of clean water was inserted into the vagina and flushed back and forth two to three times using an eyedropper. The flushed fluid was then dropped on a slide. After air-dried, the smear was examined under the microscope for the existence of leukocyte, nucleated epithelial cell and cornified epithelial cell. All vaginal smears were stained with Leu stain and examined again under the microscope. The numbers of each type of cell in the stained smears were then recorded for use in future calculation.

It is mentioned in section 2 that change in the cell type follows closely the cyclic change in the reproductive endocrines. In the present experiment, the daily recorded fraction of the number of the cornified epithelial cell (C) out of the total number of cornified epithelial cell plus leukocyte (L), i.e., $C/(C+L)$, is then taken as the single-variable time series that typifying the dynamical behavior of the reproductive endocrine system of mice.

4. Time series analysis

Figure 1 shows a typical experimental time series $s(n)$ formed by the daily-recorded values $C/(C+L)$ taken from a mouse. The power spectrum of the fluctuating sequence is given in Fig.2. The spectrum shows a broad-band distribution, no apparent periodic structure is discerned in the plot. The broad peak appears near the frequency 0.2 indicates that the average period of the estrous cycle of the mouse is around 5 days. The scalar time series $s(n)$ is to be used to generate the embedding space of the system of interest via an embedding scheme. The most popular embedding technique is the time-delay coordinates method [11] in which the coordinates of the embedding space are constructed from the vector

$$[s(n), s(n+T), s(n+2T), \cdots, s(n+(d-1)T] \quad (1)$$

In (1), T is the time lag, which is normally an integer multiple of the sampling time interval τ_s (the sampling time interval in our present experiment is 1 day), d is the dimension of the embedding space. For a proper choice of the time lag T, we adopt the concept of mutual information of Shannon [25], which states that the average mutual information $I(T)$ between data streams $s(n)$ and $s(n+T)$ in a time series can be defined as:

$$I(T) = \sum_{\substack{s(n) \\ s(n+T)}} P(s(n), s(n+T)) \log_2 \left[\frac{P(s(n), s(n+T))}{P(s(n))P(s(n+T))} \right] \quad (2)$$

In (2), $P(s(n), s(n+T))$ denotes the joint probability distribution of $s(n)$ and $s(n+T)$. The mutual information function $I(T)$ measures the extent the data in a time sequence are correlated with that at time T before and thus is a function of the time lag T. A good embedding scheme requires the greatest independence between coordinates, an obvious option for the time lag T is the time when the mutual information function first shows a minimum [26]. Figure 3 plots the average mutual information as a function of the time lag calculated from one set of experimental data. It is seen that the first minimum in $I(T)$ occurs at $T=1$. In fact, data from all mice gives the same result. It is then reasonable to fix the time lag at 1.

A proper embedding space, when interpreted geometrically, is the phase space in which all the tangles and crossings in trajectories constructed from the time series are virtually 'unfolded'. Based on this notion, a geometric scheme has been proposed [27] for determination of the minimum embedding dimension d necessary to fully unfold a time series. In the scheme, two originally close points in a d-dimensional space becomes far apart in distance when unfolded further in the d+1-dimensional space are designated as 'false nearest neighbors' (FNN). The minimum unfolding dimension under which all nearest neighbors are true neighbors, i.e., the count of FNN drops to zero, is defined as the embedding dimension d. In

Fig.4, the percentage of FNN is plotted against the unfolding dimension. Due to the presence of noise, which is often considered as a high dimensional signal in the experimental series; the count of FNN will not drop to zero literally, but instead rise again with the unfolding dimension. We then choose the embedding dimension as the one that corresponds to the minimum count of FNN. Table 1 summarizes the embedding dimension determined for each data set by this method. All data sets give consistent embedding dimension 5 or 6.

Table 1. Embedding dimensions determined from the mice data.

mouse no.	i	ii	iii	iv	v
embedding dimension d	6	5	5	5	6
mouse no.	vi	vii	viii	ix	x
embedding dimension d	5	6	5	5	6

Having determined the proper embedding dimension, a reconstructed attractor can be generated from the experimental time series in this d-dimensional embedding space. Since it is unfeasible to draw on a plane an object having a dimension more than 3; instead, we show in Fig.5 the 'projection' of the attractor in the three-dimensional space spanned by the time-delay coordinates $(s(n), s(n+1), s(n+2))$. Aperiodic nature of the attractor is apparent in this graph.

An important invariant of the reconstructed attractor is the Lyapunov exponent of the motion. The Lyapunov exponent quantifies the divergence rate of nearby trajectories. A chaotic motion is characterized by a positive Lyapunov exponent. Table 2 lists for each data set the largest Lyapunov exponent a, calculated using a scheme developed by Wolf *et al.* [28]. All data sets appear to give a positive Lyapunov exponent. Since noise also features a positive Lyapunov exponent, it is not conclusive at this point whether the experimental time series represents a chaotic signal or is dominated by a high dimensional noise.

Table 2. Lyapunov exponents calculated from the mice data.

mouse no.	i	ii	iii	iv	v
Lyapunov exponent a	0.28	0.47	0.27	0.29	0.28
mouse no.	vi	vii	viii	ix	x
Lyapunov exponent a	0.34	0.27	0.37	0.41	0.33

The other important invariant quantity characterizing the time series is the correlation dimension of the reconstructed attractor. Use of a correlation dimension to characterize a strange attractor was first proposed by Grassberger and Procaccia [29]. In general, the value of the correlation dimension calculated from a time series varies with the unfolding dimension. Figure 6 shows the correlation dimension D_C calculated from a set of data under different embedding dimension d. It is observed that the value of D_C saturates at about 3.58 after $d \geq 5$. If the time series were dominated by noise, the value of D_C would increase with the embedding dimension roughly along the 45 *deg* line in Fig.6. There are about 70% of mice in this experiment whose data exhibit such saturation in the value of the correlation dimension. A well defined correlation dimension of the reconstructed attractor, plus the positive Lyapunov exponent already listed in Table 2 suggest that the experimental time series is featured by a low-dimensional chaotic motion.

Table 3 lists the correlation dimensions calculated from the mice data. Most values are between 3 and 4, indicating that the active degree of freedom in the dynamics of the attractor is 4.

Table 3. Correlation dimensions calculated from the mice data.

mouse no.	i	ii	iv	vi
correlation dimension D_C	3.58	3.86	4.10	3.98
mouse no.	vii	ix	x	
correlation dimension D_C	3.16	3.90	3.99	

5. Discussion

It has been shown in Table 1 that the embedding dimension of the experimental series is 5 or 6. Note that the embedding dimension is determined from a geometric consideration, it is not necessarily equal to the degree of freedom of the original system. It nevertheless suggests that the function of the reproductive system of mice is described mainly by 5 or 6 physiological variables. We shall examine this aspect from the viewpoint of the endocrine function involved in the reproductive cycle.

The periodically changes of female

reproductive organs and the hormone profiles in estrus cycle are regulated by the hypothalamic - pituitary-ovarian (H-P-O) axis of the endocrine system [30]. The function of this H-P-O axis involves several hormones. Gonadotropin releasing hormone (GnRH) is secreted by hypothalamus and is stimulatory to pituitary gonadotropins secretion. FSH and LH are secreted by pituitary and are stimulatory to ovarian follicular growth and ovulation, respectively. LH also stimulates corpus luteum to secrete progesterone, and in corporation with FSH, stimulate estrogen secretion in follicles. Gonadal steroids (estrogen and progesterone) regulate pituitary gonadotropin secretion through long-loop feedback to the hypothalamus, they also exert positive and negative feedback effects directly at the level of pituitary [31]. Secreted LH and FSH exert a short-loop feedback inhibition to the hypothalamus, and may also feed back at the level of the pituitary to establish an autoinhibition effect [32]. Thus the count of the major participating hormones in this stimulation-inhibition control loop is 5 (GnRH, FSH, LH, estrogen and progesterone). Recent study discovered that another hormone named inhibin, also produced by the ovarian follicular cells, might exert a feedback inhibition specifically to FSH secretion at the level of pituitary [33]. This might account for the appearance of the sixth dimension in *d*, in some of the mice data.

The correlation dimension of the reconstructed attractor summarized in Table 3 implies that the 'active' degree of freedom of the local dynamics of the reproductive cycle is around 4. The possible physiological explanation is as follows. In this study, the length of the estrus cycle was determined by observing the morphological change of the epithelial cells in vagina smears. The morphological change of epithelial cells is directly affected by the estrogen and progesterone produced by ovarian follicular cells [34]. As described previously, the secretion profiles of estrogen and progesterone are closely related to the secretion of LH and FSH. Although GnRH can stimulate secretion of FSH and LH, it's effect on estrogen and progesterone is tied with that of FSH and LH. Furthermore, the inhibitory effect of estrogen and progesterone on GnRH is parallel to that on FSH and LH. Apparently, there is redundancy in the combined stimulation-inhibition action of GnRH, FSH and LH. The recently found extra inhibin does not affect estrogen secretion directly, and its inhibitory effect on FSH is parallel to that of estrogen. Thus the number of major independent factors that govern the dynamics of the reproductive cycle is down to 4. Of course, the above conjecture can be made substantial only after a sound mathematical model for the function of the reproductive endocrine system is proposed.

6. Concluding remarks

A dynamical-system approach has been employed to study the dynamical behavior of the estrous cycle observed in mice. Geometric techniques for reconstructing the state-space dynamics have been applied to the single-variable experimental time series sampled from the mice. Interpretation of the result regarding to the degree of freedom of the system is consistent with the physiological description of the underlying endocrine function. Also, topological properties of the reconstructed attractor suggest that the variability observed in the reproductive cycle of mice possesses the feature of a low-dimensional chaos ($D_C \leq 4$).

Present study has demonstrated the ability and usefulness of the nonlinear time series analysis via a well familiar physiological system. The ultimate goal of this research is to develop a mathematical dynamical-system model which can describe and predict qualitatively as well as quantitatively the diverse behavior of the reproductive endocrine system.

References

1. Cannon, W. B. "Organization for Physiological Homeostasis," *Physiol. Rev.*, **9**, pp. 399-431 (1929).
2. Olsen, L. F. and Degn, H. "Chaos in Biological Systems," *Quart. Rev. Biophys.*, **18**, pp. 165-225 (1985).
3. Degn, H., Holden, A. V., and Olsen, L. F. (eds.) *Chaos in Biological Systems*, Plenum Press, New York (1987).
4. Glass, L. and Mackey, M. C. *From Clocks to Chaos: The Rhythms of Life*, Princeton Univ. Press, Princeton, NJ. (1988).
5. Goldbeter, A. *Biochemical Oscillations and Cellular Rhythms*, Cambridge Univ. Press, Cambridge (1996).
6. Rosen, R. Dynamical System Theory in Biology, Volume I: Stability Theory and Its Applications, Wiley-Interscience, New York

(1970).
7. West, B. J. *Fractal Physiology and Chaos in Medicine*, World Scientific, Singapore (1990).
8. Barbi, M. and Chillemi, S. *Chaos and Noise in Biology and Medicine*, World Scientific, Singapore (1998).
9. Goldberger, A. L., Bhargava, V., West, B. J., and Mandell, A. J. "Some Observations on the Question: Is Ventricular Fibrillation 'Chaos'?," *Physica*, **19D**, pp. 282-289 (1986).
10. Goldberger, A. "Is the Normal Heartbeat Chaotic of Homeostatic?," *News Physiol. Sci.*, **6**, pp. 87-91 (1991).
11. Packard, N. H., Crutchfield, J. P., Farmer, J. D., and Shaw, R. S. "Geometry from a Time Series, " *Phys. Rev. Lett.*, **45**, pp. 712-715 (1980).
12. Takens, F. "Detecting Strange Attractors in Turbulence," in *Dynamical Systems and Turbulence*, D. A. Rand and L. S. Young, eds. Springer-Verlag, Berlin (1981).
13. Casdagli, M., Sauer, T., and Yorke, J. A. "Embedology," *J. Stat. Phys.,* **65**, pp. 579-616 (1991).
14. Yazaki, T. "Experimental Observation of Thermoacoustic Turbulence and Universal Properties at the Quasiperiodic Transition to Chaos," *Phys. Rev. E*, **48**, No. 3, pp. 1806-1818 (1993).
15. Scargle, J. D. "Studies in Astronomical Time Series Analysis. IV. Modeling Chaotic and Random Processes with Linear Filters," *Astrophys. J.*, **359**, pp. 469-482 (1990).
16. Goldberger, A. L. and Rigney, D. R. "Sudden Death Is Not Chaos," in *Dynamic Patterns in Cpmplex Systems*, J. A. S. Kelso, M. F. Schlesinger, and A. J. Mandell eds., World Scientific, Singapore (1988).
17. Schaffer, W. M. and Kot, M. "Differential Systems in Ecology and Epidemiology," in *Chaos*, A. V. Holden ed., Princeton Univ. Press, Princeton (1986).
18. Aftanas, L. I., Lotova, N. V., Koshkarov, V. I., Makhnev, V. P., Mordvintsev, Y. N., Popov, S. A. "Non-linear Dynamic Complexity of the Human EEG during Evoked Emotions," *Int. J. Psychophysiol.*, **28**, pp.63-76 (1998).
19. Scheinkman, J. and LeBaron, B. "Nonlinear Dynamics and Stock Returns," *J. Business*, **62**, pp. 311-338 (1989).
20. Nelson, J. P., Felicio, L. S., Randall, P. K., Sims, C., and Finch, C. E. "A Longitudinal Study of Estrous Cyclicity in Aging C57BL/6J mice: 1. Cycle Frequency, Length and Vaginal Cytology." *Biol. Reprod.*, **27**, pp. 327-339 (1982).
21. Flurkey, K., Randall, P. K., Sinha, Y. N., Ermini, M., Finch, C. E. "Transient Shortening of Estrous Cycles in Aging C57BL/6J mice: Effects of Spontaneous Pseudopregnancy, Progesterone, L-dihydroxyphenylalanine, and Hydergine." *Biol. Reprod.*, **36**, No. 4, pp. 949-959 (1987).
22. Nelson, J. F., Karelus, K., Felicio, L. S., Johnson, T. E. "Genetic Influences on Oestrous Cyclicity in Mice: Evidence that Cycle Length and Frequency Are Differentially Regulated." *J. Reprod. Fertil*, **94**, No. 1, pp. 261-268 (1992).
23. Allen, E. "The Oestrous Cycle in the Mouse," *Amer. J. Anat.*, **30**, pp. 297-371 (1922).
24. Cupps, P. T., Anderson, L. L., and Cole, H. H. "The Estrous Cycle," in *Reproduction in Domestic Animals*, Chapter 9, pp. 217-245 (1969).
25. Gallager, R. G. *Information Theory and Reliable Communication*, John Wiley and Sons, New York (1968).
26. Fraser, A. M. and Swinney, H. L. "Independent Coordinates for Strange Attractors from Mutual Information," *Phys. Rev. A*, **33**, pp. 1134-1140 (1986).
27. Kennel, M. B., Brown, R., and Abarbanel, H. D. I. "Determining Minimum Embedding Dimension Using a Geometrical Construction," *Phys. Rev. A*, **45**, pp. 3403-3411 (1992).
28. Wolf, A., Swift, J. B., Swinney, H. L., and Vastano, J. A. "Determining Lyapunov Exponent from a Time Series," *Physica* **16D**, pp. 285-317 (1985).
29. Grassberger, P. and Procaccia, I. "Characterization of Strange Attractors," *Phys. Rev. Lett.* **50**, pp. 346-349 (1983).
30. Edqvist, L. E. and Stabenfeldt, G. H. "The Endogenous Control of Reproductive Processes," in *Reproduction in Domestic Animals*, G. J. King ed., Elsevier Science Publishers, New York (1993).
31. Stumpf, W. E. and Sar, M. "Steroid Hormone Target Cells in the Periventricular Brain: Relationship to Peptide Hormone Producing Cells," *Fed. Proc.*, **36**, pp. 1973-1977 (1977).
32. Pattritti-Laborde, N. Wolfsen, A. R., Heber, D., and Odell, W. D. "Site of Short-Loop Feedback for Luteinizing Hormone in the Rabbit," *J. Clin. Invest.*, **64**, pp. 1066-1069 (1979).

33. Depaolo, L. V., Bicsak, T. A., Erickson, G. F., Shimasaki, S., Ling, N. "Follistatin and Activin: A Potential Intrinsic Regulatory System within Diverse Tissues," *Proc. Soc. Exp. Biol. Med.*, **198**, No. 1, pp. 500-512 (1991).
34. Mehta, R. R., Jenco, J. M., Gaynor, L. V., Chatterton, R. T. Jr. "Relationships between Ovarian Morphology, Vaginal Cytology, Serum Progesterone, and Urinary Immunoreactive Pregnanediol during the Menstrual Cycle of the Cynomolgus Monkey," *Biol. Reprod.*, **35**, No. 4, pp. 981-986 (1986).

Figures

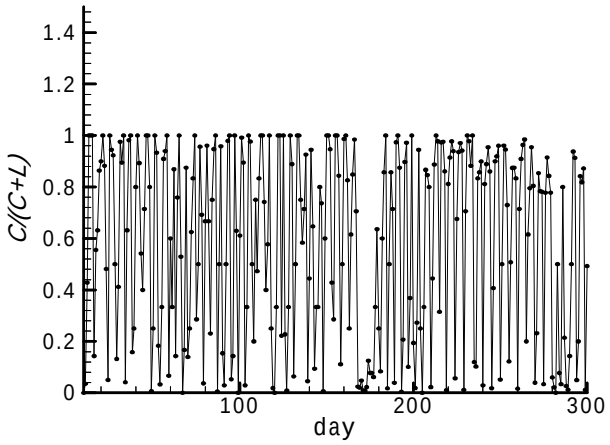

Fig.1 Daily-recorded values of cell numbers ratio.

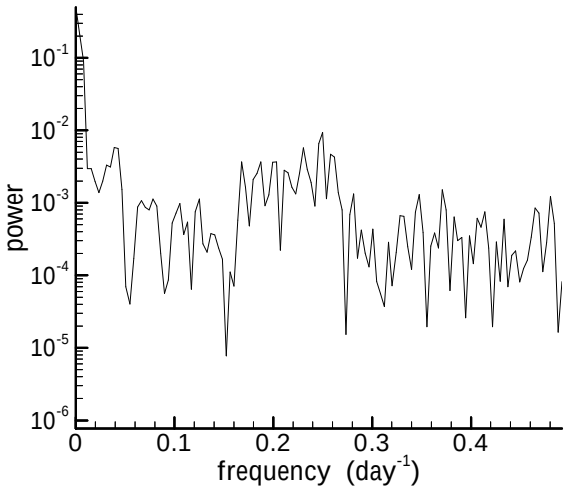

Fig.2 Typical power spectrum of the experimental time series.

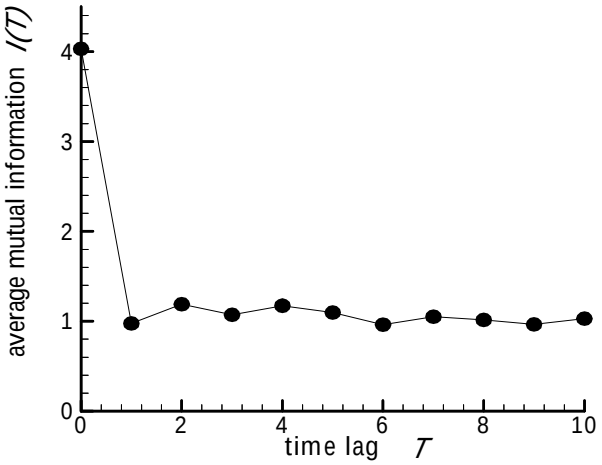

Fig.3 Average mutual information $I(T)$ vs. time lag T.

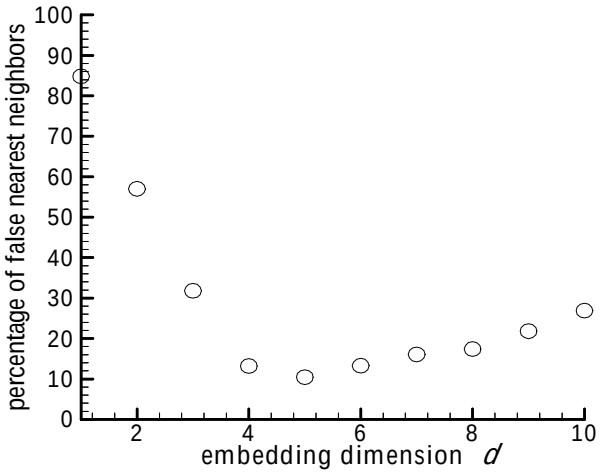

Fig.4 Percentage of false nearest neighbors vs. embedding dimension.

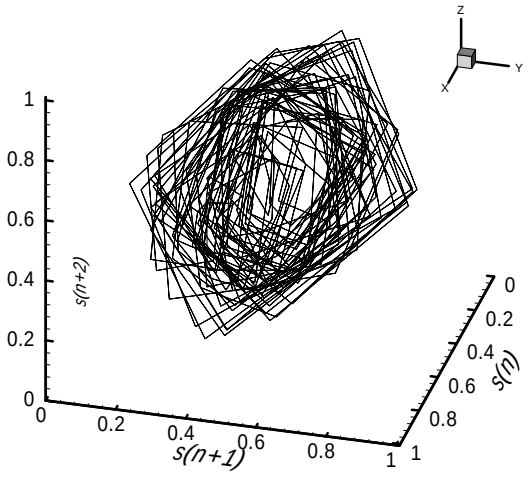

Fig.5 Projection of trajectories onto a three-dimensional state space constructed by time-delay coordinates.

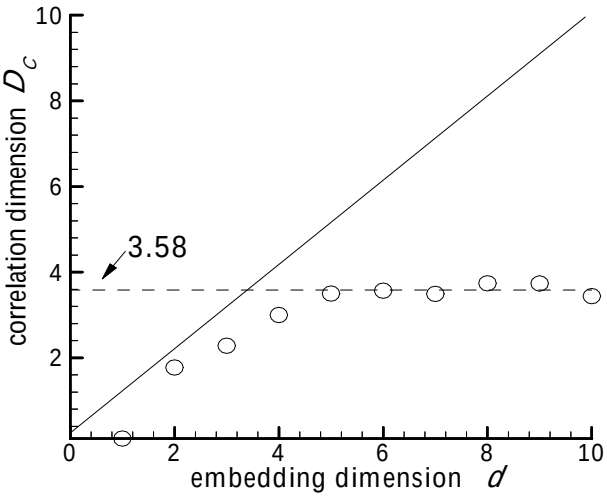

Fig.6 Correlation dimension of the attractor calculated under various embedding dimensions.